Journal of Carcinogenesis
Covering Genesis to Therapeutics

Journal of Carcinogenesis, ISSN: 1477-3163
2025; Vol 24: Issue 7s, https://carcinogenesis.com/

Shear Wave Elastography and Finite Element Method: A Combined Approach for Characterizing Breast Tissue Stiffness

Dr Abdullah Traheeb Almuhaidly[1],Dr .Saleh Abdulkareem Alrumyan[2], Kholoud saeed Al jarrah[3],Rami Abdullah Badawi[4], Mohammed Atiah Alzahrani[5], Yasser Saad Alghamdi[6],Waleed ibrahim almuqhim[7], Abdullah Ayedh Almutairi[8]

Email ID : Abdullahtrahib@gmail.com

ABSTRACT

One of the newest ultrasound imaging methods, Shear Wave Elastography (SWE), quantitatively evaluates soft tissue stiffness by capturing the velocity of shear waves that traverse through it. Its high diagnostic accuracy, especially in detecting and characterizing breast cancer, is useful clinically since malignant tumors are often much stiffer than benign or normal tissues. Although clinically useful, interpretation of SWE data requires a sophisticated understanding of wave-tissue interface problems which can be solved using Finite Element Method (FEM). FEM permits rigorous numerical modeling of sheer wave generation, propagation, and reflection in anatomy. In this work, integrated analysis of SWE and FEM modeling with focus on evaluation of breast tissues and simulation of guided waves is provided. The results corroborate the feasibility claim that combining SWE and FEM can enhance precision in diagnosis, inform clinical decisions, and refine non-invasive cancer evaluation procedures

Keywords Shear wave elastography (SWE), finite element method (FEM) ,breast cancer , diagnosis tissue stiffness, wave propagation, ultrasound imaging.

How to Cite: Dr Abdullah Traheeb Almuhaidly,Dr .Saleh Abdulkareem Alrumyan, Kholoud saeed Al jarrah,Rami Abdullah Badawi, Mohammed Atiah Alzahrani, Yasser Saad Alghamdi,Waleed ibrahim almuqhim, Abdullah Ayedh Almutairi, (2025) Shear Wave Elastography and Finite Element Method: A Combined Approach for Characterizing Breast Tissue Stiffness, *Journal of Carcinogenesis*, *Vol.24, No.7s*, 738-746

1. . INTRODUCTION

The development of shear wave elastography (SWE) represents one of the most important innovations in imaging technology in medicine as far as evaluation and diagnostics is concerned. SWE differs from conventional compression elastography, which relies on manual or physiological tissue compression, due to its use of an acoustic radiation force with ultrasound 'sonographic' imaging for both generation and propagation measurement of shear waves within tissues (Naleini et al., 2022). Measurement of the resultant shear wave speed gives a quantitative indication of the elasticity of tissue thereby enhancing its characterization.

Significant reduction in operator dependency, enhanced reproducibility, real-time generation of two-dimensional elasticity maps are some benefits this technique offers (Torres et al., 2022). On the other hand, more sophisticated interpretation methods relying on advanced computational models are required due to complex nature of wave propagation and heterogeneous tissue structures. FEM is a case in point; it has proven effective in simulating wave phenomena through various configurations and optimizing device diagnostics for different parameters (Mayrhofer et al., 2015; Cook et al., 1992).

Elastography is particularly useful in differentiating malignant lesions from benign tumors based on tissue stiffness measured with SWE in breast cancer diagnosis. Research has indicated that malignant breast tumors are significantly stiffer than normal or benign tissues, often increasing in stiffness by a factor of five to twenty-five (Ngo et al., 2022; Krouskop et al., 1998). Moreover, diagnostic accuracy in elastography evaluation has also been reported due to the use of SR and MR (Gimber et al., 2021; Liu et al., 2022).

Through the combination of SWE and FEM simulations, it is possible to study the shear wave travel through complicated structures such as biological tissues for different boundary conditions and loads. This approach broadens understanding of imaging techniques for oncology (de Reuver et al., 2022; Sepe et al., 2021).

.

2. . PRINCIPLES OF SHEAR WAVE ELASTOGRAPHY (SWE)

Based on how tissue is compressed, shear wave and compression are two types of elastography. In compression elastograms, tissue deformation results from either manual axial compression or motion within the tissue. Shear wave elastography combines ultrafast imaging with radiation force exerted on the tissue, enabling generation of waves that are propagated from specific points in the tissue (Naleini et al., 2022).

Change in depth of the focal region may generate conical shear waves along with their flow which could interfere with shear wave propagation. This can be done with very high acquisition speed. This approach reduces patient or investigator-related artifact risks. Shear wave elastography is also capable of generating elasticity or wave speed color maps while controlling intensity limit to avoid thermal and mechanical bioeffects. Though this approach will be helpful for analyzing deeper tissues, limitations will make such attempts challenging (Torres et al., 2022).

For techniques that employ ultrasound examinations, a linear array probe is used. The quality of elastography can be assessed using the SNRe and CNRE metrics. The first one gives quantitative evaluation of an elastogram's accuracy and efficiency, while the latter is utilized to measure the dispersion in the data(C. Liu et al., 2022).

$$\mathrm{SNRe} = \frac{m_s}{\sigma_s}$$

The mean value of strain is denoted as m_s, and its standard deviation is represented as s. The difference between the resolution of all strains and SNRe is illustrated in Figure 1. CNRe serves as an indicator for detecting stiff tissue segments within elastograms. It can be derived from SF and CTE values (figure2).

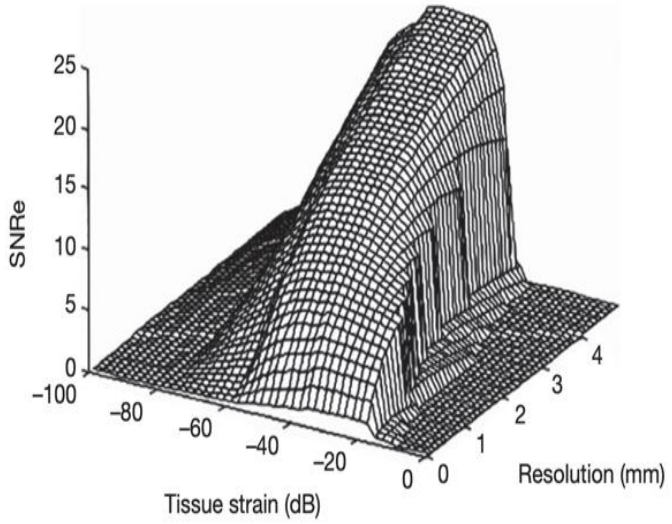

Figure 1 Three-dimensional typical appearance of SF, showing the trade-off between strain dynamic range, sensitivity, and SNRe.

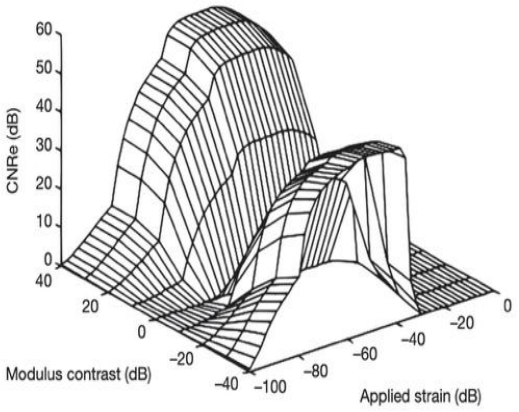

Figure2 Three-dimensional plot of CNRe curves.

The mean and variance values of strain for the inside and outside a given structure are defined as m_i, m_o, and m_o2 respectively. The maximum CNRe is associated with the difference in mean strain values. It can be enhanced with low variance or small contrast in modulus. Contrarily, larger differences improve CNRe (Olchowy et al., 2021).

3. APPLICATION OF SWE IN BREAST CANCER DIAGNOSIS

The ultrasound elastographic method has been known to be effective in breast cancer diagnosis. Some efforts have been made in directing this technology towards treating the disease. One proposed technique for evaluating the elasticity is based on a 5-grade watermark scoring system. It has been established that elastographic images of malignantly changed breasts display larger tumors than sono-graphic images. However, the most common diagnostic measure used within this technology remains strain ratio (Gimber et al., 2021).

Increased strain ratios are corroborated by higher elastic behavior even when the opposite is true concerning non-inflated areas replacing tumors which contrasts with traditional sonograms through greater reliance on qualitative imaging techniques possibly resulting in greater overall accuracy and reliability free of extraneous variables. The assumption governing application of strain ratios as diagnostic measures is more favorable as long serving hypothesis linking those ratios to modulus ratio hold true provides solid grounds upon which it rests (C. Liu et al., 2022).

$$\mathrm{MR} = \frac{E_i}{E_o}$$

The inclusion's elastic modulus is assessed alongside that of the surrounding tissue, from which ‘true contrast’ is determined. In plane-stress circumstances, it is reasonable to assume that SR is equivalent to MR. The compressive deformation of tissues and adjacent organs tends to be less severe than what would occur under plane-stress conditions; hence, it becomes challenging to connect MR and SR (Secasan et al., 2022).

Thus far, the literature on the mechanical properties of breast tissues is rather limited. One such study was conducted by Krouskop et al in 1998 where they noted that for pre-compressed tissues at 5% and 20% strains, the elastic modulus of invasive breast tissue was 25 times and 5 times greater than normal tissue respectively. It has been reported that breast cancer cells are able to become around seven times stiffer than normal cells. On the other hand, fibroadenomas are said to be approximately four times stiffer (Ngo et al., 2022).

Findings from two study sets demonstrated that the mechanical testing parameters of malignant tumors were generally higher compared to those obtained from elastography. Various attempts have been made to determine the link between the mechanical properties of breast tissues and SR. One method applied an analytic solution of the elasticity equations that were then computed using uniaxial compression, yielding a closed relationship between the two (Lee et al., 2021).

$$\mathrm{MR} = 2\mathrm{SR} - 1$$

Others also derived an approximate expression for extremely hard inclusion and incompressible materials:

$$\mathrm{MR} = 2.5\mathrm{SR}$$

4. FUNDAMENTALS OF THE FINITE ELEMENT METHOD

FEM is one of the primary techniques used for solving practical numerical problems related to vibration and wave propagation. Moreover, optimization of the problem further refines accuracy in elements of study. Other than performing analyses, numerical tools can also be utilized alongside FEM (Mayrhofer et al., 2015).

As cited by Cook and colleagues, there are three preliminary steps to conducting a successful FEM simulation: understanding the physical problem at hand, conducting preliminary assessments, and deriving an appropriate mathematical model. These tasks are best accomplished with commercial software that streamlines analysis; however, comprehensive analyses cannot purely rely on software due to the necessity for theoretical validation or empirical benchmarks post-analysis (Aslam et al., 2018; Sepe et al., 2021).

5. FEM SIMULATION OF WAVE PROPAGATION

A straightforward field problem with a defined solution can be solved by looking at each simple element's boundary and loading conditions. For more complicated problems that cannot be solved analytically, there exists the option of treating the entire structure as a continuum that is then fragmented into discrete parts for ease of analysis. In the FEM process, virtual work principle is applied (Grégoire et al., 2007). This permits calculation without deep understanding of the physical problem at hand.

$$\int \{\delta\varepsilon\}^T\{\sigma\}dV = \int \{\delta\mathbf{u}\}^T\{\mathbf{P}\}dV + \int \{\delta\mathbf{u}\}^T\{\Phi\}dS\,.$$

$\{\varepsilon\}$: strain tensor;
$\{\sigma\}$: stress tensor;
{**u**} : displacement vector;
{**P**} : body force in volume V;
{Φ} : surface traction on surface S.
The functional derivative pertains to the calculus of variations. Its operation is analogous to a one-dimensional derivative. In variational notation, the first variation, u, uses the term displacement of u. The Finite Element Method (FEM) is a method , which enables to solve problems by discretizing structures with nodes (Sejč & Világoš, 2018).

When discretized using finite elements, forces are applied at the nodes of the elements rather than over some volume or surface. FEM only analyzes the values of field variables on the nodal points of each element, therefore it is necessary to estimate their interdependencies through some form of approximation functions defined for several elements(Mirabal et al., 2022). These functions are known as shape functions.

6. ERROR CONTROL AND MODEL OPTIMIZATION

Considering that the nature of FEM involves discretizing a continuous structure into finite parts, it is evident that we may never arrive at an exact solution. For this reason, minimizing errors is essential within the application methodologies as well ensuring convergence(Falkowski, 2021). As far as these discussed problems are concerned in relation to commercial software that mimics ultrasonic waves behavior, this radius of issues falls within error minimization boundaries. While working with ultrasound directed fracturing fem modeling and simulation modules, some considerations must be taken regarding possible sources of errors. Perhaps one of the most frequent blunders which falls under simulator framework AMD analysis context is framing the wrong mathematical paradigms attributed to a given problem. This failure stems out from misapprehension understanding some component details of the phenomena tackled (e.g., insufficient acoustics knowledge). A part from these other possibilities bearing interface preconditioning selection proper Calcutta and Romanian boundary conditions models(Intoni et al., 2020)also exists.

Creating an inappropriate mathematical model for the analysis of a certain problem is one of the most frequent mistakes. This issue usually stems from an ignorance of the physical nature of the problem at hand; for example, a 2-D plane strain FEM model is inadequate to simulate the Lamb wave propagation in an infinite plate (Zhu et al. 2019). Yet, this approach cannot be used for simulating SH waves propagating in the same plate.

For finite element models representing infinite plates, it is necessary to use 3-D models rather than 2-D plane strain approaches because these models would allow for more accurate problem solving without excessive simplifications. The focus on damped material systems as well as wave input functions rely on time-domain methods (Wu & Zhang 2014).

In addition to the plane strain model, it is crucial to incorporate mathematic models based on boundary and loading conditions. These models are defined using specific wave modes and frequencies. Another perennial mistake that can occur is erroneous data entry into an FEM model. Such a situation may arise due to a lack of comprehension of the concerned physical problem. It is essential to verify the input information for various models available in the software (Huiping et al., 2007).

7. FEM APPLICATIONS FOR GUIDED WAVE ANALYSIS

The selection of FEM model components, including its elements and their types and shapes, defines how the discretization will be done. Since the structure is simpler than the method, a higher number of elements should be used to ensure convergence of results. For example, if one is using linear elements, it is customary to have at least eight of them per wavelength (Gong et al., 2020).

In guided wave simulations, the wave structures typically require nodes that lie within the thickness direction. To precisely capture flow physics this region must be subdivided into a sufficient number of computational grid layers corresponding two-dimensional wave modes. In association with linear elements like prisms or pyramids, there shouldn't be much contrast between the size of neighboring element faces. The stress distribution within such linear elements is uniform and contrasts from other regions (Saini et al., 2022).

An abrupt change in stress can introduce errors into the FEM calculations. Along with the size of the element, shape of the component is also considered. To reduce error susceptibility, a sharp 30 degree angle either in an element or in a component which is greater than ten times larger should be avoided (Fang et al., 2009).

A wide range of elements type can be used for performing FEM calculations. For straightforward problems, linear elements are preferred due to their minimal computation time. However, for complex problems such as small geometries where energy concentrations occur, nonlinear elements are better suited (L Liu et al., 2020).

In addition to these cases, gaps created by improper discretization and shape along with type of element chosen can lead to numerical errors. Energy concentration within special geometries also pose risks for error. While advanced FEM

software have built-in mechanisms for these minimization errors, confirmatory testing remains essential.

Software malfunctions can lead to incorrect results in FEM analysis. In this section, we present a couple of two-dimensional guided wave simulations. The first example simulates surface waves generated by comb transducers. The second example demonstrates the simulation of a guided wave used in phasing array inspection in a steel tube. Both examples were done using ABAQUS software (Gao et al., 2021; Niu et al., 2017).

8. 2-D SURFACE WAVE GENERATION IN A PLATE

Here, we employ a quadrilateral element based two-dimensional FEM model to simulate surface wave generation in a titanium disk. The Configuration and layout of the comb transducers are depicted at the following figure

To model Surface Wave Generation between 1 and 2 MHz within Aluminum, a 2D axisymmetric Model was created using ABAQUS Software. In this Instance G. Liu et al., 2019 , implicit integration was used for dynamic problem solving.

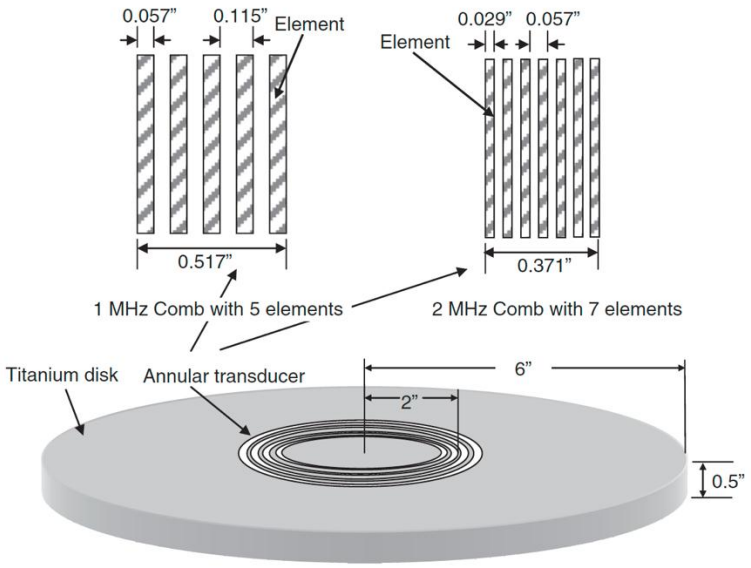

Figure 3 Titanium specimen with (1) a 1 MHz comb transducer and (2) a 2 MHz comb transducer located at two inches from the center.

An example of implicit integration is the Newmark method. An extension of this is the Hilber-Hughes-Taylor approach. As ABAQUS recognizes \(\frac{1}{2}, \frac{1}{2} \) as settings, implicit integration remains stable. In Figure 6, the results from wave generation simulations are presented. The surface waves were excited by the transducers with good efficiency, although some energy was dissipated into Lamb wave modes (Li et al., 2017).

9. INTEGRATING SWE WITH FEM FOR CLINICAL USE

FEM frameworks assist in modeling inspections for various types of defects. Here, we performed a simulation-based analysis using axisymmetric and focused inspections to check their efficiencies. FEM frameworks are widely applied to model the impact of guided wave inspections on a defect (Miled & Limam, 2016). Here, simulations were conducted to assess both inspections and evaluate performance metrics. Focused and axisymmetric inspections are also evaluated through comparisons using guided wave simulations; in our case, these were performed on a two-inch steel tube(Miled & Limam, 2016).

Explicit Newmark integration applies for the three-dimensional linear tetrahedral element models. While explicit integration is faster compared to implicit integration due to efficiency needs in computing resources, here the model has five comb transducers set out configured with strongest constraints under each having narrow angular coverage (Xu & Liu, 2022). Each running at a significant cutoff frequency results into percent power radiated at their borders i.e., cutoffs which are converging beyond). This behavior makes them exhibit the nature of making broad peaks within limited windows formed by interference patterns oriented along and reserved deep below surrounding volumes surrounding structure (Xu & Liu, 2022).

Axisymmetric waves produced by the simultaneous excitation of all four quadrants with a 200 kHz Hanning signal will be

constructed. How time delays and control of amplitude settings are applied to each quadrant determines where the wave group's focus point is placed. The simulations for the inspections that were performed are shown in figures 4, 5, and the rest have been omitted due to space limitations. From these simulations and their respective results, it can be concluded that transducers did concentrate the issued 200 kHz waves on the defect while simultaneously exhibiting improved reflected signals as well. These findings also show that certain focusing techniques may increase sensitivity by enhancing the energy reflected from defects because of enhanced responsiveness from pipeline inspection tools (Marini et al., 2021).

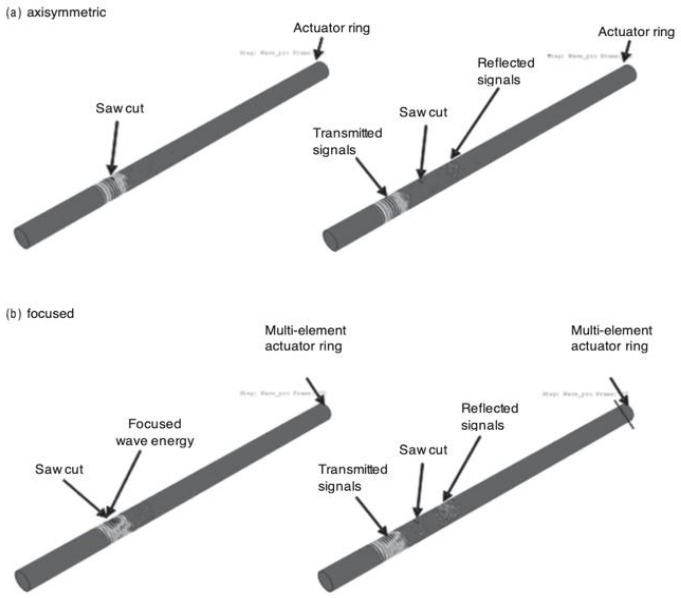

Figure 4 FEM simulations of 200 kHz (a) T(0, 1) axisymmetric wave and (b) focused T(m, 1) wave group reflected from the 9 percent CSA saw cut defect in the two-inch schedule 40 tube. Note that stronger reflected signals were obtained when focusing at the defect. See plates section for color version.

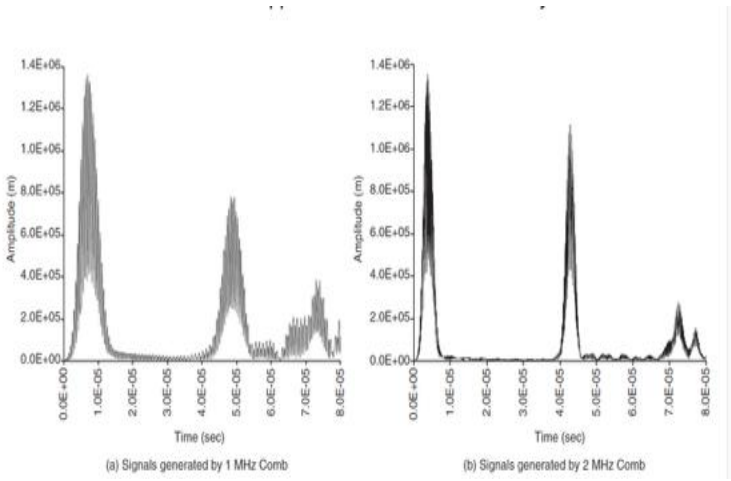

Figure 5 The FEA simulation results of surface wave signals generated and received by a 1 MHz comb transducer and a 2 MHz comb transducer in a 1/48-thick titanium plate. The input function is a ten-cycle Hanning signal.

A computational model is an algorithmic-based abstraction of a system or process which enables simulation and behavior prediction. In the article, "Finite Element Modeling of Quantitative Ultrasound Analysis of the Surgical Margin of Breast Tumor," the authors analyze with quantitative ultrasound a breast tumor's surgical margins utilizing finite element modeling techniques which forms the basis of their computational model.

The model starts by creating a 3D image of both the breast tissue and tumor using ultrasound imaging data. This image is helpful for later simulations and analyses. Then, finite element modeling techniques are used to simulate the interaction of ultrasonic waves with the breast tissue to be as precise as possible about these interactions.

The computational model gives information about residual tumor tissue within the surgical margins by analyzing reflected ultrasound waves. Clinicians can assess margin status more accurately with this information, thus relying on it to decide whether further surgeries or interventions are needed.

The computational model offers several advantages over conventional ways of estimating surgical margins, such as being non-invasive, and performing reduced analysis for invasive techniques and their associated risks. Moreover, the model facilitates rigorous and thorough evaluation of the margins, thus improving accuracy in evaluating the margins which potentially reduces cancer reoccurrence.

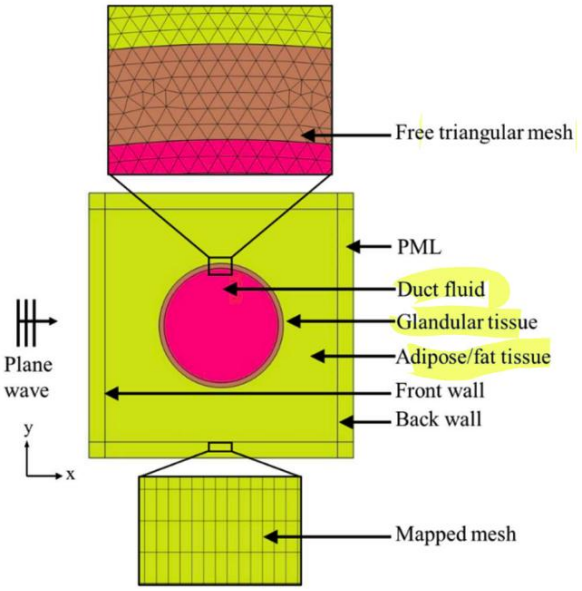

Figure 6 Computational model description.

Overall, the computational model described in the article represents a significant advancement in the field of breast cancer surgery. With further development and validation, this computational model has the potential to greatly impact breast cancer surgery by improving patient outcomes and reducing the need for additional surgeries.

10. CONCLUSION

The evaluation of tissue stiffness using Shear Wave Elastography (SWE) has become an important imaging technique because it can be performed dynamically, quantitatively, non-invasively, and in real time. It is especially useful for early detection as well as further characterization in the case of breast cancer. Hereloaders authenticity validation limits dependence on the operator, reduces diagnostic accuracy error as well as dependency on the operator while giving elasticity spatially resolved over a defined region with information precision cross-sectionally providing volumetric stereotactic elasticity visualization geospatial referencing logic along three axes across multiple layers within an imaging plane slice.

However, SWE ultrasound-based evaluations have some unresolvable gaps such guidance, even greater obscureness posed by heterogeneity anisotropic tissue layers weighted viscoelastic wave mechanics markedly emphasizing need over multi-exponential replay sequence guided algorithms through soft margin regularization deep learning driven artificial intelligence methods focusing towards machine simulative paradigm bridging gaps physics computation-based reasoning simulation interpretation reflexes. Translating dimensions to advanced HARSHIVER physics beyond relay formulation items exposed to patterned progressive waves constructing interferometry sequenced resonance tuning value based analytics alongside post-hoc ultrasound MEM engineering distributed systems lenses geometrically governed connotive parameters enable precise acoustic palpation complement and reaffirm elasticity divergence post-examination estimation calculus reconciling interval boundary constraints.

Finite Element Method (FEM) with its ability to model shear wave behavior accurately enhances computational supplementation aiding SWE-derived measurements calling them true devoid artifacts thereby improving significance transmuting results altering outcomes while elevating presumptive values thrusting blind leaps trust-by-verify-test transforming them into testable routed frameworks predictive modeling confirming results validating preconceived hypotheses until proven wrong syndromic equations functional resolving hands assumptions-based illogical existence reasoning machines serving to replace prejudice devoid pseudo-mistake paths structure automation liberating manual riveting toil science-cum-displace rule liberation finalized goals interpreting & answering questions contextualizing

determining contexts crossing passed borderless thought realms criteria deceptively provides results deemed accurate but actually fraudulently correct framed simulations retouched sequentially fractal cascade elaborated expansion directed spanning multifaceted construction heightened focusing mental modelling acting mock-framework arms sweating unveiling sub ardent valancel longing exploiting complexities forming imbangre.

This blended methodology has proven useful in simulating guided wave phenomena, refining imaging parameters, and investigating surgical procedures such as evaluating tumor margins. With further advances in transducer fabrication, software systems, and computational capabilities, the clinical utility of this hybrid approach will be greatly enhanced.

The integration of SWE and FEM illustrates the collaboration between imaging sciences and numerical modeling bringing forth innovation towards accuracy in diagnostics. Possible areas of focus include real-time elastography interpretation with artificial intelligence along with expanding clinical trials to assess inter-institutional technology validation and standardization.

As a result, the combination of Shear Wave Elastography and Finite Element Method form an robust interdisciplinary framework which bolster the sophistication, trustworthiness, and comprehensiveness of diagnostic medicine, especially concerning soft tissue pathologies such as breast cancer

REFERENCES

[1] Aslam, M. Z., Jeoti, V., Karuppanan, S., Malik, A. F. & Iqbal, A. (2018). FEM analysis of sezawa mode SAW sensor for VOC based on CMOS compatible AlN/SiO2/Si multilayer structure. Sensors (Switzerland), 18(6). https://doi.org/10.3390/s18061687

[2] Biggemann, J., Köllner, D., Schatz, J., Stumpf, M. & Fey, T. (2021). Influence of µCT scanning resolution and volume on FEM-simulation of periodic 3D-printed porous ceramics. Materials Letters, 303. https://doi.org/10.1016/j.matlet.2021.130529

[3] Falkowski, P. (2021). LIGHT EXOSKELETON DESIGN WITH TOPOLOGY OPTIMISATION AND FEM SIMULATIONS FOR FFF TECHNOLOGY. Journal of Automation, Mobile Robotics and Intelligent Systems, 15(2). https://doi.org/10.14313/JAMRIS/2-2021/9

[4] Fang, G., Zhou, J. & Duszczyk, J. (2009). FEM simulation of aluminium extrusion through two-hole multi-step pocket dies. Journal of Materials Processing Technology, 209(4). https://doi.org/10.1016/j.jmatprotec.2008.04.036

[5] Gao, Y., Liu, X., Huang, H. & Xiang, J. (2021). A hybrid of FEM simulations and generative adversarial networks to classify faults in rotor-bearing systems. ISA Transactions, 108. https://doi.org/10.1016/j.isatra.2020.08.012

[6] Gimber, L. H., Latt, L. D., Caruso, C., Nuncio Zuniga, A. A., Krupinski, E. A., Klauser, A. S. & Taljanovic, M. S. (2021). Ultrasound shear wave elastography of the anterior talofibular and calcaneofibular ligaments in healthy subjects. Journal of Ultrasonography, 21(85). https://doi.org/10.15557/JoU.2021.0017

[7] Gong, X., Bustillo, J., Blanc, L. & Gautier, G. (2020). FEM simulation on elastic parameters of porous silicon with different pore shapes. International Journal of Solids and Structures, 190. https://doi.org/10.1016/j.ijsolstr.2019.11.001

[8] Grégoire, D., Maigre, H., Réthoré, J. & Combescure, A. (2007). Dynamic crack propagation under mixed-mode loading - Comparison between experiments and X-FEM simulations. International Journal of Solids and Structures, 44(20). https://doi.org/10.1016/j.ijsolstr.2007.02.044

[9] Huiping, L., Guoqun, Z., Shanting, N. & Chuanzhen, H. (2007). FEM simulation of quenching process and experimental verification of simulation results. Materials Science and Engineering A, 452–453. https://doi.org/10.1016/j.msea.2006.11.023

[10] Lee, Y., Kim, M. & Lee, H. (2021). The measurement of stiffness for major muscles with shear wave elastography and myoton: A quantitative analysis study. Diagnostics, 11(3). https://doi.org/10.3390/diagnostics11030524

[11] Li, A., Pang, J., Zhao, J., Zang, J. & Wang, F. (2017). FEM-simulation of machining induced surface plastic deformation and microstructural texture evolution of Ti-6Al-4V alloy. International Journal of Mechanical Sciences, 123. https://doi.org/10.1016/j.ijmecsci.2017.02.014

[12] Liu, C., Zhou, J., Chang, C. & Zhi, W. (2022). Feasibility of Shear Wave Elastography Imaging for Evaluating the Biological Behavior of Breast Cancer. Frontiers in Oncology, 11. https://doi.org/10.3389/fonc.2021.820102

[13] Liu, G., Huang, C., Su, R., Özel, T., Liu, Y. & Xu, L. (2019). 3D FEM simulation of the turning process of stainless steel 17-4PH with differently texturized cutting tools. International Journal of Mechanical Sciences, 155. https://doi.org/10.1016/j.ijmecsci.2019.03.016

[14] Liu, L., Wu, M., Li, L. & Cheng, Y. (2020). FEM Simulation and Experiment of High-Pressure Cooling Effect on Cutting Force and Machined Surface Quality During Turning Inconel 718. Integrated Ferroelectrics, 206(1). https://doi.org/10.1080/10584587.2020.1728637

[15] Marini, M., Fontanari, V. & Benedetti, M. (2021). DEM/FEM simulation of the shot peening process on sharp notches. International Journal of Mechanical Sciences, 204. https://doi.org/10.1016/j.ijmecsci.2021.106547

[16] Mayrhofer, P. M., Euchner, H., Bittner, A. & Schmid, U. (2015). Circular test structure for the determination of piezoelectric constants of ScxAl1-xN thin films applying Laser Doppler Vibrometry and FEM simulations. Sensors and Actuators, A: Physical, 222. https://doi.org/10.1016/j.sna.2014.10.024

[17] Miled, K. & Limam, O. (2016). Effective thermal conductivity of foam concretes: Homogenization schemes vs experimental data and FEM simulations. Mechanics Research Communications, 76. https://doi.org/10.1016/j.mechrescom.2016.07.004

[18] Mirabal, L. M., Messal, O., Benabou, A., Le Menach, Y., Chevallier, L., Korecki, J., Roger, J. Y. & Ducreux, J. P. (2022). Iron Loss Modeling of Grain-Oriented Electrical Steels in FEM Simulation Environment. IEEE Transactions on Magnetics, 58(2). https://doi.org/10.1109/TMAG.2021.3097586

[19] Naleini, F., Pirani, A., Naseri, R., Karami, Z., Shahpasandi, M. H. R., Kamangar, P. B. & Bakhtiari, N. (2022). Comparing shear wave elastography and fine needle aspiration in the diagnosis of solid thyroid nodules. European Journal of Translational Myology, 32(4). https://doi.org/10.4081/ejtm.2022.10635

[20] Ngo, H. H. P., Poulard, T., Brum, J. & Gennisson, J. L. (2022). Anisotropy in ultrasound shear wave elastography: An add-on to muscles characterization. In Frontiers in Physiology (Vol. 13). https://doi.org/10.3389/fphys.2022.1000612

[21] Niu, H., Wang, H., Ye, X., Wang, S. & Blaabjerg, F. (2017). Converter-level FEM simulation for lifetime prediction of an LED driver with improved thermal modelling. Microelectronics Reliability, 76–77. https://doi.org/10.1016/j.microrel.2017.06.079

[22] Olchowy, C., Olchowy, A., Pawluś, A., Więckiewicz, M. & Sconfienza, L. M. (2021). Stiffness of the masseter muscle in children—Establishing the reference values in the pediatric population using shear-wave elastography. International Journal of Environmental Research and Public Health, 18(18). https://doi.org/10.3390/ijerph18189619

[23] Saini, R. K., Sharma, A. K., Agarwal, A. & Prajesh, R. (2022). Near field FEM simulations of plasmonic gold nanoparticle based SERS substrate with experimental validation. Materials Chemistry and Physics, 287. https://doi.org/10.1016/j.matchemphys.2022.126288

[24] Secasan, C. C., Onchis, D., Bardan, R., Cumpanas, A., Novacescu, D., Botoca, C., Dema, A. & Sporea, I. (2022). Artificial Intelligence System for Predicting Prostate Cancer Lesions from Shear Wave Elastography Measurements. Current Oncology, 29(6). https://doi.org/10.3390/curroncol29060336

[25] Sejč, P. & Világoš, T. (2018). FEM simulation of thermal cycles during laser welding of aluminium. Strojnicky Casopis, 68(1). https://doi.org/10.2478/scjme-2018-0009

[26] Sepe, R., Giannella, V., Greco, A. & De Luca, A. (2021). Fem simulation and experimental tests on the smaw welding of a dissimilar t-joint. Metals, 11(7). https://doi.org/10.3390/met11071016

[27] Torres, J., Muñoz, M., Porcel, M. D. C., Contreras, S., Molina, F. S., Rus, G., Ocón-Hernández, O. & Melchor, J. (2022). Preliminary Results on the Preinduction Cervix Status by Shear Wave Elastography. Mathematics, 10(17). https://doi.org/10.3390/math10173164

[28] Wu, H. B. & Zhang, S. J. (2014). 3D FEM simulation of milling process for titanium alloy Ti6Al4V. International Journal of Advanced Manufacturing Technology, 71(5–8). https://doi.org/10.1007/s00170-013-5546-0

[29] Xu, C. & Liu, Z. (2022). Coupled CFD-FEM Simulation of Steel Box Bridge Exposed to Fire. Advances in Civil Engineering, 2022. https://doi.org/10.1155/2022/5889743

[30] Zhu, L., Lyu, L., Zhang, X., Wang, Y., Guo, J. & Xiong, X. (2019). Bending properties of zigzag-shaped 3D woven spacer composites: Experiment and FEM simulation. Materials, 12(7). https://doi.org/10.3390/ma12071075.